

Ongoing Meteor Work

Activity Analysis of the 1996 Geminids

Jürgen Rendtel and Rainer Arlt

An analysis of 19604 Geminids seen in 1996 is given. The maximum occurred at $\lambda_{\odot} = 262^{\circ}15 \pm 0^{\circ}20$ (December 13, 20^h UT) with ZHR = 115 ± 10 . The profile of the population index shows a decrease of the r -value during the maximum. Small-scale features in the ZHR-profile could not be found.

1. Introduction

Another successful Geminid year was logged by observers from several continents in 1996 with a very thin waxing Moon not interfering with the maximum of the meteor shower. In total, 119 observers recorded 19604 Geminids in 491 man hours. We are very grateful to the following observers who contributed to the analysis below:

Rainer Arlt (ARLRA, 6^h65), Adrian Paulo Arquiola (ARQAD, 4^h33), Joseph D. Assmus (AS-SJO, 11^h60), Lars Bakmann (BAKLA, 2^h50), Luc Bastiaens (BASLU, 0^h92), Jim Bedient (BEDJI, 3^h75), Luis R. Bellot (BELLU, 10^h66), Orlando Benítez Sánchez (BENOR, 2^h24), Felix Bettonvil (BETFE, 3^h67), Michael Boschat (BOSMI, 1^h34), Lieve Bresseleers (BRELI, 3^h45), Salvatore Calafiore (CALSA, 0^h86), Koen Clement (CLEKO, 2^h70), Tim Cooper (COOTI, 5^h44), Celina Raquel Cudiciotti (CUDCE, 4^h34), Alberto Darias (DARAL, 2^h79), Mark Davis (DAVMA, 14^h42), Johan de Hert (DE JO, 0^h92), Goedele Deconink (DECGO, 2^h70), Adrián Fernández Vigo (FERAD, 1^h84), David Antonio Fernández Vigo (FERND, 1^h29), Keiiti Fukui (FUKKE, 2^h70), Tositake Fukuhara (FUKTO, 1^h83), Yosinori Fuyube (FUYYO, 3^h18), M. Inmaculada Gómez Fernández (GOMIN, 1^h00), Roberto Gorelli (GORRO, 1^h91), Peter S. Gural (GURPE, 5^h12), Michael Hann (HANMI, 1^h50), Yukiti Hattori (HATYU, 1^h50), David Hernandez (HERDA, 0^h90), Veerle Herrygers (HERVE, 2^h55), Richard Huziak (HUZRI, 1^h50), Kiyoshi Izumi (IZUKI, 3^h08), Carl Johannink (JOHCA, 4^h05), Ron Johnson (JOHRO, 5^h88), Geoffrey Johnstone (JOHGE, 0^h60), Aram Karalič (KARAR, 1^h05), Niladri Kar (KARNI, 6^h31), Jana Kasparova (KASJA, 1^h55), Atusi Kisanuki (KISAU, 1^h42), Miroslav Kopal (KOPMI, 1^h55), Detlef Koschny (KOSDE, 1^h32), Ralf Koschack (KOSRA, 6^h42), Gotfred M. Kristensen (KRIGO, 4^h08), Alexander Kupco (KUPAL, 1^h62), Marco Langbroek (LANMA, 8^h99), Alberto Latini (LATAL, 4^h00), Sebastiano Leggio (LEGSE, 1^h00), Inge Leyssens (LEYIN, 1^h88), Alister Ling (LINAL, 4^h49), Robert Lunsford (LUNRO, 20^h17), Ake Lysell (LYSAK, 0^h33), Katuhiko Mameta (MAMKA, 3^h66), Martin Nick (MARNI, 1^h63), Takuya Maruyama (MARTA, 3^h83), Yukihisa Matumoto (MATYU, 1^h67), Alastair McBeath (MCBAL, 6^h37), Bruce McCurdy (MCCBR, 5^h00), Tom McEwan (MCETO, 3^h00), Norman McLeod (MCLNO, 34^h08), Carl B. Miller (MILCA, 2^h16), Dante Militano (MILDA, 4^h33), Koen Miskotte (MISKO, 9^h46), Hidekazu Mizoguchi (MIZHI, 3^h10), Sirko Molau (MOLSI, 4^h94), Koiti Nagano (NAGKO, 0^h75), Dragana Okolić (OKODR, 2^h35), Jens O. Olesen (OLEJE, 1^h00), Urška Pajer (PAJUR, 1^h67), Gregg Pasterick (PASGR, 1^h94), John Penner (PENJO, 1^h56), Jorge Pena Pinedo (PENJR, 1^h78), Tim Polfiet (POLTI, 7^h43), Tim Printy (PRITI, 3^h33), Luis Quintana Armas (QUILU, 2^h60), Andreas Rendtel (RENAN, 17^h28), Jürgen Rendtel (RENJU, 25^h06), Rigney Ian (RIGIA, 1^h62), Natalia Risiglione (RISNA, 4^h33), Mike Rosseel (ROSMI, 2^h95), John Ruddy (RUDJO, 5^h00), Javier Sanchez (SANJA, 1^h34), Sergio Sánchez Jiménez (SANSE, 1^h34), Branislav Savic (SAVBR, 2^h82), René Scurbecq (SCURE, 5^h03), Miguel Serra Martin (SERMI, 2^h22), Francisco Sevilla (SEVFR, 11^h81), Yasuo Shiba (SIBYA, 3^h67), Hiroyuki Sioi (SIOHI, 1^h83), Manuel Solano Ruiz (SOLMA, 2^h11), Carlos F. Sosa (SOSCA, 4^h33), George Spalding (SPAGE, 6^h50), Ulrich Sperberg (SPEUL, 2^h00), Umberto Mule Stagno (STAUM, 3^h50), Plamen Stoichev (STOPL, 3^h00), Wesley Stone (STOWE, 2^h91), Máximo Svárez Tejera (SVANX, 0^h63), David Swann (SWADA, 1^h95), Yoshihiro Takahashi (TAKYO, 3^h17), Taylor Melvyn (TAYME, 3^h50), Marko Toivonen (TOIMA, 2^h83), Josep M. Trigo Rodriguez (TRIJO, 1^h55), Yoshiaki Uyama (UYAYO, 2^h59), Erwin Van Balleghoy (VANER, 1^h82), Frans Van Loo (VANFA, 2^h00), Hendrik Vandenbruaene (VANHE, 6^h06), Michel Vandeputte (VANMC, 6^h71), Valentin Velkov (VELVA, 4^h51), Cis Verbeeck (VERCI, 3^h60), Daniel Verde (VERDA, 2^h60), Jan Verbert (VERJN, 3^h03), Damian Wacker (WACDA, 4^h33), Michael Webb (WEBMC, 0^h77), Graham Winstanley (WINGR, 1^h00), Yasuo Yabu (YABYA, 5^h26), Hiromiti Yosidome (YOSHI, 1^h00), Ilkka Yrjölä (YRJIL, 2^h28), George Zay (ZAYGE, 16^h02), Irena Zivkovic (ZIVIR, 1^h55).

2. Data reduction and perception coefficients

The large amount of data allowed the computation of a population index profile which is then used to calculate the individual zenithal hourly rates (ZHR) of each observing period. Magnitude distributions used for population index determinations should contain at least 20 meteors, and at least 3 meteors in at least 5 consecutive magnitude classes after being corrected with perception probabilities (the probability to detect a meteor of given magnitude; do not mix them up with perception coefficients which are described later). The faintest magnitude class should be at least 2^m brighter than the limiting magnitude since the perception probabilities at the faint end of the magnitude distribution introduce large errors because of the small number of meteors compared to the large correction necessary. Perception probabilities and computation of population indices and their errors are taken from [1].

Different window lengths for the average r -profile were used: Until $\lambda_{\odot} = 260^{\circ}5$ (December 12, 5^h UT), a window size of 2^o0 (48 hours) shifted by 1^o0 was used; in the period $\lambda_{\odot} = 260^{\circ}5$ –262^o8 (December 12, 5^h–December 14, 11^h UT), the window had a length of 0^o5 (12 hours) shifted by 0^o25; and after $\lambda_{\odot} = 262^{\circ}8$, we used a window of 2^o0 duration shifted by 1^o0 again.

The individual ZHRs are computed by

$$\text{ZHR} = \frac{r^{6^{m5}-lm-\Delta lm} F n}{T_{\text{eff}} \sin h_{\text{R}}}$$

where r is the population index, lm is the limiting magnitude, Δlm is perception correction (see below), F is the correction for observing field obstructions, n is the number of Geminids seen during T_{eff} , which is the effective observing time (excluding any times during which the observer was not facing the sky, e.g., recording times), and h_{R} is the altitude of the Geminid radiant.

Like the r -profile, the ZHR-profile was created from the individual values with different averaging windows: until $\lambda_{\odot} = 260^{\circ}5$, a window of 2^o0 shifted by 1^o0 was used; in the interval $\lambda_{\odot} = 260^{\circ}5$ –262^o8 the length of the window was 0^o4 (10 h) shifted by 0^o2; after $\lambda_{\odot} = 262^{\circ}8$, the window was again 2^o0 shifted by 1^o0. The individual ZHRs were only considered for the ZHR-profile if the average radiant altitude exceeded 20^o, and the total correction $C = r^{6^{m5}-lm-\Delta lm} F / \sin h_{\text{R}}$ was smaller than 5.0. The individual ZHRs are weighted with $1/C$.

A comprehensive set of perception coefficients was derived in an analysis of Geminid returns of the last 9 years [2]. The coefficients are obtained by comparing Geminid ZHRs of individual observers with the average during relatively short periods of almost constant activity. The perception coefficients are expressed by differences in the limiting magnitude Δlm .

3. The r -profile and ZHR-profile

The profile of the population index r derived from 1996 Geminid observations is shown in Figure 1. The first value is based on very few magnitude distributions and covers the whole period $\lambda_{\odot} = 259^{\circ}$ –261^o. The population index fell significantly lower than in 1991 [3] and 1993 [4]. Maximum and minimum of the r -profile (neglecting the uncertain far-end values) coincide with the ascending and descending part of the activity curve. A high population index before the ZHR maximum and a low r -value after the peak is shown by both the 1991 and 1996 data. This behavior is not visible in the 1993 r -profile, though it lacks data after $\lambda_{\odot} = 262^{\circ}3$. The continuous decrease of r from 2.4 before the ZHR peak to $r = 1.9$ after the rate maximum shows the mass sorting within the meteoroid stream. During the ascending rate branch, the Earth encounters a region containing a rather small portion of larger meteoroids (of order 10 mg), while their portion increases until after the actual ZHR peak. This feature is generally known by meteor photographers because of the higher success rate after the peak compared to the ascending branch. It may also explain the impression of different maximum times in years with strong moonlight interference and other years.

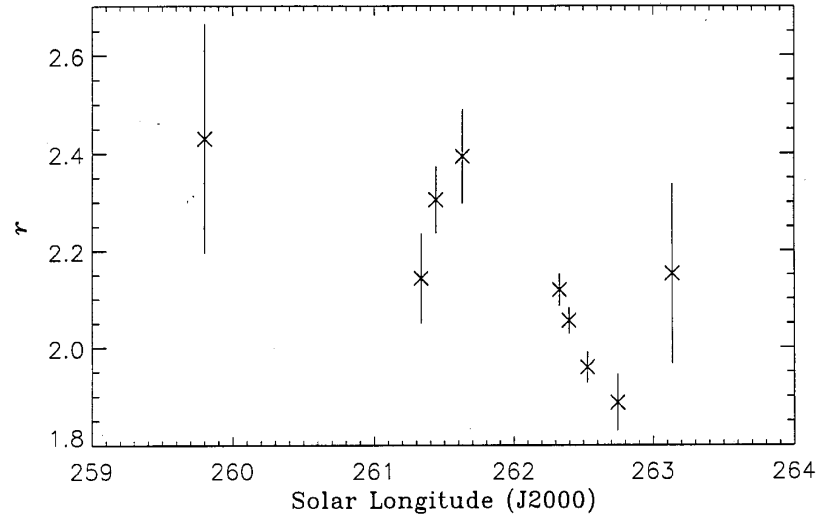


Figure 1 – Profile of the population index r of the 1996 Geminids. The first value is an average of only 3 observations before $\lambda_{\odot} = 261^{\circ}$.

The ZHR-profile of the 1996 Geminids is shown in Figure 2. The profile is very smooth and does not show any peculiarities.

A profile with higher time resolution during the maximum applying only observing periods with $T_{\text{eff}} \leq 2^{\text{h}}0$ does not show a significant fine structure different from a round summit either (Figure 3).

Observations from East Asian longitudes mainly covering $\lambda_{\odot} = 261^{\circ}9-262^{\circ}1$ result in much larger scatters of the averages. Most of the Japanese observers have higher than average perception coefficients which is also expressed in their high sporadic rates. Hence, we only consider the whole summit to be the activity maximum occurring at $\lambda_{\odot} = 262^{\circ}15 \pm 0^{\circ}20$ (December 13, 20^h UT) with $\text{ZHR} = 115 \pm 10$.

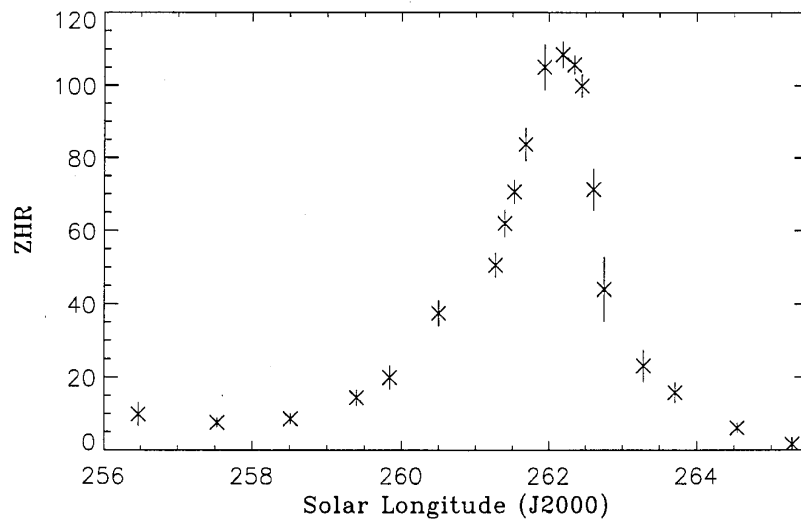


Figure 2 – ZHR-profile of the 1996 Geminids.

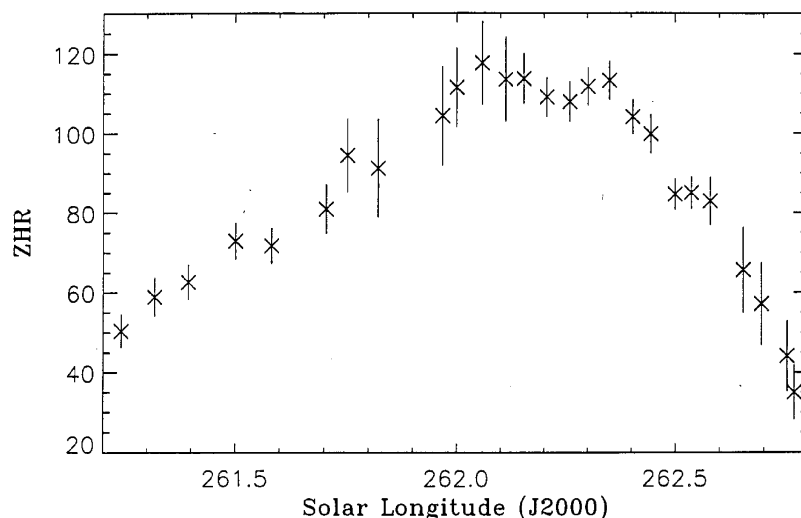


Figure 3 - Fine structure of the Geminid maximum. Only observing periods with $T_{\text{eff}} \leq 2^{\text{h}}$ were used; the window for averaging was $0^{\circ}20$ (4.8 hours), shifted by $0^{\circ}1$ until $\lambda_{\odot} = 261^{\circ}8$, and $0^{\circ}10$ (2.4 hours), shifted by $0^{\circ}05$ for the right part of the graph.

The peak rate agrees well with previous occurrences of the Geminids; Table 1 gives an overview of the last reliably analyzed Geminid maxima since 1988.

Table 1 - Time and ZHR of Geminid maxima derived from global analyses since 1988. The values were taken from [2-6].

Year	λ_{\odot}	ZHR
1988	262°1	130
1990	262°26	110
1991	262°3	110
1993	262°1	130
1996	262°15	115

The full width at half maximum of the Geminid peak is $1^{\circ}4$ in solar longitude, or 31 hours. This agrees well other returns like 1990 ($1^{\circ}25$), 1991 ($1^{\circ}6$), and 1993 ($1^{\circ}4$). The 1996 data confirm a plateau activity: the high activity of $ZHR > 100$ lasted for about 12 hours (December 13/14, $15^{\text{h}}-3^{\text{h}}$ UT). We may conclude that the 1996 activity fits well in the stable behavior of the Geminid meteor shower.

References

- [1] R. Koschack, J. Rendtel, "Determination of Spatial Number Density and Mass Index from Visual Observations (II)", *WGN* 18:4, August 1990, pp. 119-140.
- [2] P. Brown, J. Rendtel, "The Current Geminid Meteoroid Stream", *in preparation*, 1997.
- [3] J. Rendtel, R. Arlt, P. Brown, "The 1991 Geminid Meteor Shower", *WGN* 21:1, February 1993, pp. 19-28.
- [4] R. Arlt, J. Rendtel, "A Global Analysis of the 1993 Geminids", *WGN* 22:5, October 1994, pp. 167-172.
- [5] P. Roggemans, "The Geminid Meteor Stream in 1988", *WGN* 17:6, December 1989, pp. 229-239.
- [6] P. Roggemans, R. Koschack, "The 1990 Geminids", *WGN* 19:5, October 1991, pp. 184-193.